Front. Phys. 13(5), 137308 (2018)
https://doi.org/10.1007/s11467-018-0806-y

RAPID COMMUNICATION

Quantum anomalous Hall effect and giant Rashba spin-orbit splitting in graphene system co-doped with boron and 5*d* transition-metal atoms

Xinzhou Deng[1,2], Hualing Yang[3], Shifei Qi[3,1,†], Xiaohong Xu[3], Zhenhua Qiao[1,2,‡]

[1] *ICQD, Hefei National Laboratory for Physical Sciences at Microscale, and Synergetic Innovation Center of Quantum Information and Quantum Physics, University of Science and Technology of China, Hefei 230026, China*
[2] *CAS Key Laboratory of Strongly-Coupled Quantum Matter Physics, and Department of Physics, University of Science and Technology of China, Hefei 230026, China*
[3] *School of Chemistry and Materials Science, Shanxi Normal University, Linfen 041004, China*
Corresponding authors. E-mail: †qisf@sxnu.edu.cn, ‡qiao@ustc.edu.cn
Received May 23, 2018; accepted June 5, 2018

Quantum anomalous Hall effect (QAHE) is a fundamental quantum transport phenomenon in condensed matter physics. Until now, the QAHE has only been experimentally realized for Cr/V-doped $(Bi, Sb)_2Te_3$ but at an extremely low observational temperature, thereby limiting its potential application in dissipationless quantum electronics. By employing first-principles calculations, we study the electronic structures of graphene co-doped with 5*d* transition metal and boron atoms based on a compensated *n*–*p* co-doping scheme. Our findings are as follows: i) The electrostatic attraction between the *n*- and *p*-type dopants effectively enhances the adsorption of metal adatoms and suppresses their undesirable clustering. ii) Hf-B and Os-B co-doped graphene systems can establish long-range ferromagnetic order and open larger nontrivial band gaps because of the stronger spin-orbit coupling with the non-vanishing Berry curvatures to host the high-temperature QAHE. iii) The calculated Rashba splitting energies in Re–B and Pt–B co-doped graphene systems can reach up to 158 and 85 meV, respectively, which are several orders of magnitude higher than the reported intrinsic spin-orbit coupling strength.

Keywords graphene, quantum anomalous Hall effect, spin-orbit coupling

PACS numbers 73.22.Pr, 75.50.Pp, 75.70.Tj

1 Introduction

Significant discoveries related to the quantum anomalous Hall effect (QAHE), which is a new quantum state of matter in condensed matter physics, have been reported in recent years. The QAHE exhibits quantized Hall conductance in the absence of an external field, which arises from strong spin-orbit coupling (SOC) combined with breaking of the time-reversal symmetry owing to intrinsic magnetization [1–4]. It is a topologically nontrivial phase characterized by a finite Chern number and chiral edge states within the bulk band gap. The chiral edge states are robust against backscattering and are promising for application to devices that require low power consumption.

To date, the QAHE has been theorized to occur in systems such as Mn-doped HgTe quantum wells [5], thin-film topological insulators (TIs) [6], silicene [7–10], half-hydrogenated Bi honeycomb monolayers [11], and graphene-based systems [12–16]. Graphene and TIs are candidate materials for engineering the QAHE because of their unique linear Dirac dispersion [17–19] and the existence of mature technologies for growing samples. TIs are superior to graphene because they have stronger SOC, thereby narrowing the search for suitable materials for realizing the QAHE. Magnetism can be effectively induced in TIs by doping them with magnetic atoms [6, 20–23]. The QAHE was first observed experimentally in Cr- and V-doped thin films at extremely low tem-

*arXiv: 1805.02230.

peratures [24–27]. Recently, the QAHE at temperatures above 50 K via n–p co-doping in Sb_2Te_3 using vanadium–iodine has been theoretically proposed [28], which has inspired significant experimental advances in exploiting high-temperature QAHE [29].

Graphene has become a promising candidate material for achieving the QAHE because of its extraordinary electrical property, unique honeycomb lattice, and relatively mature technologies for sample growth [17, 19]. However, pristine graphene possesses a very small nontrivial band gap because of its extremely weak intrinsic SOC [30, 31]. Therefore, various measures such as hydrogen deposition [32] have been proposed to enhance the extrinsic SOC in graphene. In particular, periodic adsorption of transition metal (TM) atoms has been theoretically suggested as an effective way to enhance SOC in graphene [12, 33]; however, its experimental realization is currently very difficult. A subsequent study observed that random adsorption of TM atoms can eliminate the intervalley scattering associated with periodic adsorption [34]. However, the adsorption energies of metal atoms on graphene are usually very low and metal atoms tend to form clusters even at low temperatures [35, 36], indicating that the long-range ferromagnetic (FM) order may not survive as expected although some elements, such as Bi cluster-decorated graphene, exhibit enhanced SOC [37]. Thus, it is important to explore new strategies to solve the aforementioned problems. Recently, it was confirmed that n–p co-doping is effective for enhancing the adsorption of TM atoms on graphene, leading to FM graphene [38–41]. Furthermore, the n–p co-dopants can help preserve the Dirac nature of the charge carriers.

In this article, by using first-principles calculations in the realm of density functional theory, we propose a versatile approach for achieving the QAHE based on a compensated n–p co-doping scheme. This method was initially introduced to achieve p doping in ZnO [42, 43] and to narrow the band gap of TiO_2 [44, 45]; more recently, it was proposed in the context of diluted magnetic semiconductors [38, 39, 41, 46, 47], which can also significantly enhance the adsorption of TM atoms on graphene. Furthermore, the successful fabrication of B-substituted graphene also inspired our proposal [48]. In addition, owing to their strong atomic SOC, heavy $5d$ TMs might cause larger QAHE gaps in related systems. Therefore, we study the electronic and topological behaviors of $5d$ TM–B co-doped graphene systematically by utilizing n–p co-doping. First, we determine that the electrostatic attraction between the n- and p-type dopants effectively enhances the adsorption of the metal adatoms and suppresses their undesirable clustering. The results reveal that the magnetic coupling of all $5d$ TM–B pairs shows a Ruderman–Kittel–Kasuya–Yosida type spatial fluctuation, with only Hf and Os being able to form long-range FM order. When SOC is considered, Hf–B and Os–B co-doping can both open up a global band gap to facilitate the QAHE with non-vanishing Berry curvatures. Subsequently, we calculated the Rashba splitting energies in Re–B and Pt–B co-doped graphene systems as approximately 158 and 85 meV, respectively, which are several orders of magnitude larger than the reported intrinsic SOC strength.

2 Computational methods

The calculations were performed using the projector augmented-wave formalism of density functional theory [49] as implemented in the Vienna ab initio simulation package (VASP) [50, 53, 54]. For exchange correlation, we used the Perdew–Burke–Ernzerhof [55, 56] functional. The graphene sheet was modeled (i) with a 4×4 supercell with a 20 Å vacuum in the vertical direction for the adsorption calculations and (ii) with a 7×7 supercell with a 20 Å vacuum to estimate the magnetic interaction between two TM–B pairs. We used the optimized lattice constant of graphene $a_0 = 2.46$ Å, which is consistent with the experimental value, in all our calculations. When optimizing the geometry, the positions of all atoms were allowed to relax and the atomic structures were optimized fully until the Hellmann–Feynman forces on each ion were less than 0.02 eV/Å. The plane-wave energy cutoff was set as 500 eV with an energy precision of 10^{-4} eV. For the 4×4 (resp. 7×7) supercell, the Brillouin zone was sampled using a 15×15 (resp. 5×5) Γ-centered k-point grid. The Gaussian smearing method was used with a smearing width of 0.1 eV. The adsorption energies of the $5d$ TM adatoms on the B-substituted graphene sheet were estimated using

$$E_{\mathrm{ad}} = E_{\mathrm{tot}} - E_{\mathrm{atom}} - E_{\mathrm{gra+B}},$$

where E_{tot}, E_{atom}, and $E_{\mathrm{gra+B}}$ are the energies of the $5d$ TM–B co-doped graphene system, an isolated TM atom, and B-substituted graphene, respectively.

3 Results and discussion

We begin by studying the adsorption of a single $5d$ TM adatom on the graphene monolayer. We consider three highly symmetric adsorption sites, namely a carbon-atom top site, a carbon–carbon bridge site, and a hollow site. From Table 1, we observe that two stable adsorption sites (data in parentheses in Table 1) are obtained for Hf, Ta, W, and Re, whereas only one adsorption site is obtained for Os, Ir, and Pt. In the case of an Au adatom on graphene, three stable adsorption sites (one bridge,

Table 1 Magnetic moments (M) of TM atoms (TM = Hf, Ta, W, Re, Os, Ir, Pt, and Au) adsorbed on B-substituted (pristine) graphene at three possible adsorption sites. A blank entry indicates that the corresponding configuration is unstable.

Atom	Site	Move		$M(\mu_B)$	
	bridge	no	(yes)	0.56	
Hf	hollow	no	(no)	2.71	(3.11)
	top	no	(no)	0.37	(1.50)
	bridge	no	(yes)	2.00	
Ta	hollow	no	(no)	3.82	(3.68)
	top	yes	(no)		(2.99)
	bridge	yes	(yes)		
W	hollow	no	(no)	3.29	(2.31)
	top	yes	(no)		(5.79)
	bridge	yes	(yes)		
Re	hollow	no	(no)	0.00	(0.89)
	top	no	(no)		
	bridge	yes	(yes)		
Os	hollow	no	(no)	1.00	(1.97)
	top	no	(yes)	3.00	
	bridge	yes	(no)		(0.95)
Ir	hollow	no	(yes)	1.72	
	top	no	(yes)	1.93	
	bridge	no	(no)	0.00	(0.00)
Pt	hollow	yes	(yes)		
	top	yes	(yes)		
	bridge	yes	(no)		(0.86)
Au	hollow	yes	(no)		(0.84)
	top	no	(no)	0.00	(0.85)

one hollow, and one top) are obtained. Regarding the magnetic properties of a 5d TM adatom on pristine graphene, no magnetic moment appears in the case of Pt-adsorbed graphene. However, owing to the various adsorption configurations, various magnetic moments are obtained with the other 5d TM adatoms adsorbed on graphene. These differing configurations and magnetic moments reflect the differing charge transfer when these 5d TM adatoms are adsorbed onto graphene at different sites. Our results also show that the hollow site is the most favored adsorption site except for Pt and Ir, for which the bridge site is preferred. This finding is consistent with the findings of previous theoretical studies [15]. Our calculations also show that the largest adsorption energy among the various 5d TM adatoms (namely that for Ta) is less than 2 eV on pristine graphene. This relatively weak binding between graphene and each of these 5d TM adatoms, in addition to the small diffusion barrier, results in fast adatom migration and clustering. We show that co-doping with B is effective for suppressing these undesirable effects as follows.

As mentioned above, the relatively low adsorption energies of TM-doped graphene cannot prevent the fast migration of adatoms and clustering with other adatoms adsorbed on graphene. The 5d TM adatoms are n-type dopants in graphene, whereas B adatoms (occupying the same row as carbon in the periodic table with only one less electron) are p-type dopants. Therefore, a 5d TM adatom will be located close to a B adatom because of the strong n–p electrostatic attraction between them. Previous studies have also shown that B co-doping is effective for suppressing the present undesirable effects [38, 41]. To demonstrate this phenomenon, we calculated the adsorption energies of the 5d TM adatoms from Hf to Au after B co-doping. As shown in Fig. 1, the adsorption energies exhibit an enhancement of ∼1 eV compared with those on pristine graphene, indicating a strong attractive interaction between TM and B. We observed that most of the 5d TM adatoms yield the strongest binding at the hollow site after co-doping except for Pt and Au, for which the bridge and top sites are preferred, respectively. Such strong attraction helps pin the TM adatoms close to B, thereby preventing their migration and clustering on graphene. Regarding the magnetic moment of graphene co-doped with B and 5d TM adatoms, Table 1 indicates that no magnetic moment appears when using Re, Pt, or Au. In fact, B co-doping results in more charge transfer, and therefore, the magnetic moment is different from that in the case of using only 5d TM adatoms. Therefore, the abovementioned findings confirm that n–p co-doping distributes 5d TM adatoms uniformly and stably on B-substituted graphene.

The results presented thus far show that 5d-TM–B co-doping enhances the stability of TM adatoms on graphene significantly, thereby providing the essential prerequisites for achieving enhanced SOC and realizing the QAHE in graphene. Ferromagnetism is another crucial requirement to realize the QAHE in n–p co-doped graphene, and hence, we subsequently consider the mag-

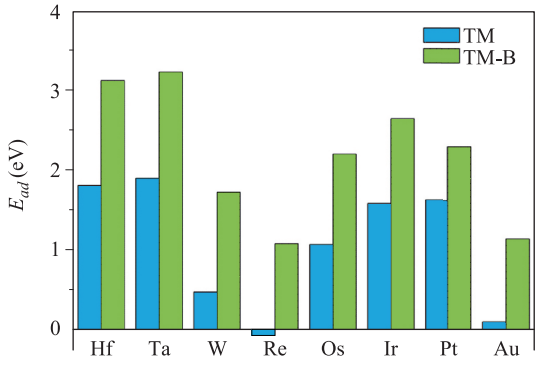

Fig. 1 Adsorption energies of 5d TM adatoms on pristine graphene (blue) and B-substituted graphene (green).

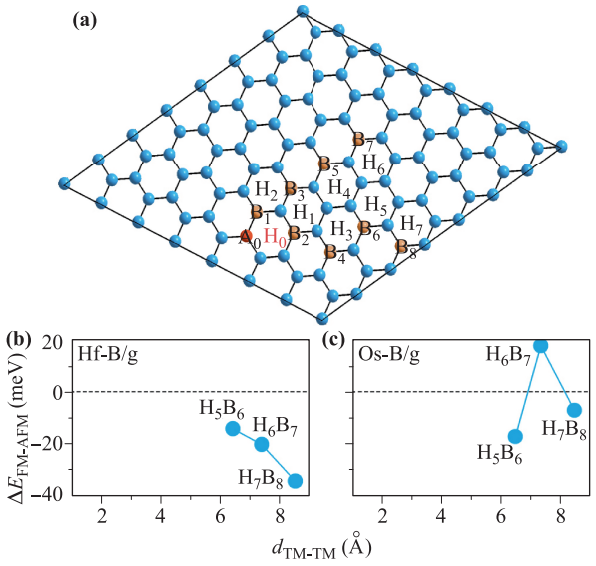

Fig. 2 **(a)** A 7×7 graphene supercell. H_0-H_7 represent the hollow sites for TM adsorption, A_0 and B_1-B_8 represent the B-substituted "A" site and "B" sites of carbon atoms in graphene, respectively. **(b) (c)** Magnetic coupling between two TM–B pairs vs. their separation. One pair is fixed at H_0A_0 and the other one moves from H_1B_2 to H_7B_8, as illustrated in (a).

netic interaction between two TM–B pairs in a 7×7 graphene supercell. As shown in Fig. 2(a), one TM adatom is fixed at H_0 and paired with a B atom at A_0. The other TM adatom moves from H_1 to H_7, whereas its partner B co-dopant remains at its nearest neighbor. The magnetic interaction between the two TM–B pairs at a given separation is evaluated by calculating the total energy difference between the FM and the antiferromagnetic (AFM) configurations of the two TM moments. We observe that the first to fourth nearest-neighbor configurations are unstable owing to the surprisingly large attraction between the two $5d$ TM adatoms even though their corresponding adsorption energies increase after B co-doping. However, it remains possible to realize long-range ferromagnetism because configurations with larger separations between the two co-dopants appear. As shown in Figs. 2(b) and (c), we also observe that both Hf–B and Os–B co-doped graphene systems display FM coupling at a sufficiently large TM-TM distance, indicating the existence of long-range FM order in these two systems. However, our calculations show the absence of long-range FM order in the other types of $5d$-TM–B co-doped graphene systems. Therefore, the Hf–B and Os–B co-doped graphene systems are the most promising candidates for achieving the QAHE.

The $5d$-TM–B co-doping enhances the stability of TM adatoms significantly, and the Hf–B and Os–B co-doped graphene systems can realize long-range ferromagnetism. Subsequently, to verify whether the QAHE can be realized in n–p co-doped graphene, we calculate the band structures of Hf–B and Os–B co-doped graphene. First, we examine Hf on graphene in a 4×4 supercell with and without SOC. In Fig. 3, panels (a) and (b) show the band structures of Hf-doped graphene without SOC, wherein the unique linear dispersion of pure graphene is preserved. In Fig. 3(c), a gap of ~ 35.9 meV opens at the Dirac point when SOC is activated, indicating that this gap originates from the SOC related to the adsorption of Hf adatom. The abovementioned results are consistent with those of Zhang *et al.* [15], indicating that our computational method is reliable. Subsequently, in Figs. 3(f) and (j), we show the band structures of Hf–B and Os–B co-doped graphene, respectively, without SOC. When magnetization is included, the spin-up (resp. spin-down) bands are shifted upward (resp. downward). When SOC is also activated, band gaps open at the crossing points between the spin-up and spin-down bands near the K point, as shown in Figs. 3(g) and (k), with magnitudes of 21.4 and 47.6 meV, respectively. Therefore, the QAHE might be realized in Hf–B and Os–B co-doped graphene. Notably, these opened QAHE band gaps are much larger than those observed in our previous study, where they were only approximately 10 meV in graphene systems co-doped with 3d TMs and boron adatoms.

So far, we have shown that the combined effect of SOC and FM exchange field can open up band gaps in Hf–B and Os–B co-doped graphene. Subsequently, we investigate whether such band gaps can host the QAHE via Berry curvature calculations using the expression [51, 52]

$$\Omega(\boldsymbol{k}) = -\sum_{n} f_n \sum_{n' \neq n} \frac{2\mathrm{Im}\langle\psi_{nk}|v_x|\psi_{n'k}\rangle\langle\psi_{n'k}|v_y|\psi_{nk}\rangle}{(E_{n'} - E_n)^2},$$

where n, E_n, and ψ_{nk} are the band index, eigenvalue, and eigenstate, respectively, of the n-th band. $v_{x,y}{=}\partial E/\partial k_{x,y}$ represents velocity operators in the x and y directions within the film plane, and $f_n = 1$ for all n bands below the band gap. Figures 3(g) and (k) show the distributions of Berry curvature along highly symmetric lines. Large negative peaks appear near the K points and disappear elsewhere, demonstrating nonzero Hall conductance. Therefore, our calculations confirm that these gaps can host the QAHE at higher temperatures owing to the strong SOC of $5d$ TMs.

We also present the band structures of the Re–B and Pt–B co-doped graphene systems even though they have no magnetism. The overall band structures of Re–B and Pt–B co-doped graphene with and without SOC are shown in Fig. 4. With SOC, there is no topologically nontrivial band gap. However, Figs. 4(c) and (g) show the existence of spin-orbit splitting. In contrast to Figs. 4(b) and (f) without SOC, the SOC interaction breaks the spin degeneracy of the bands of Re–B and Pt–B co-

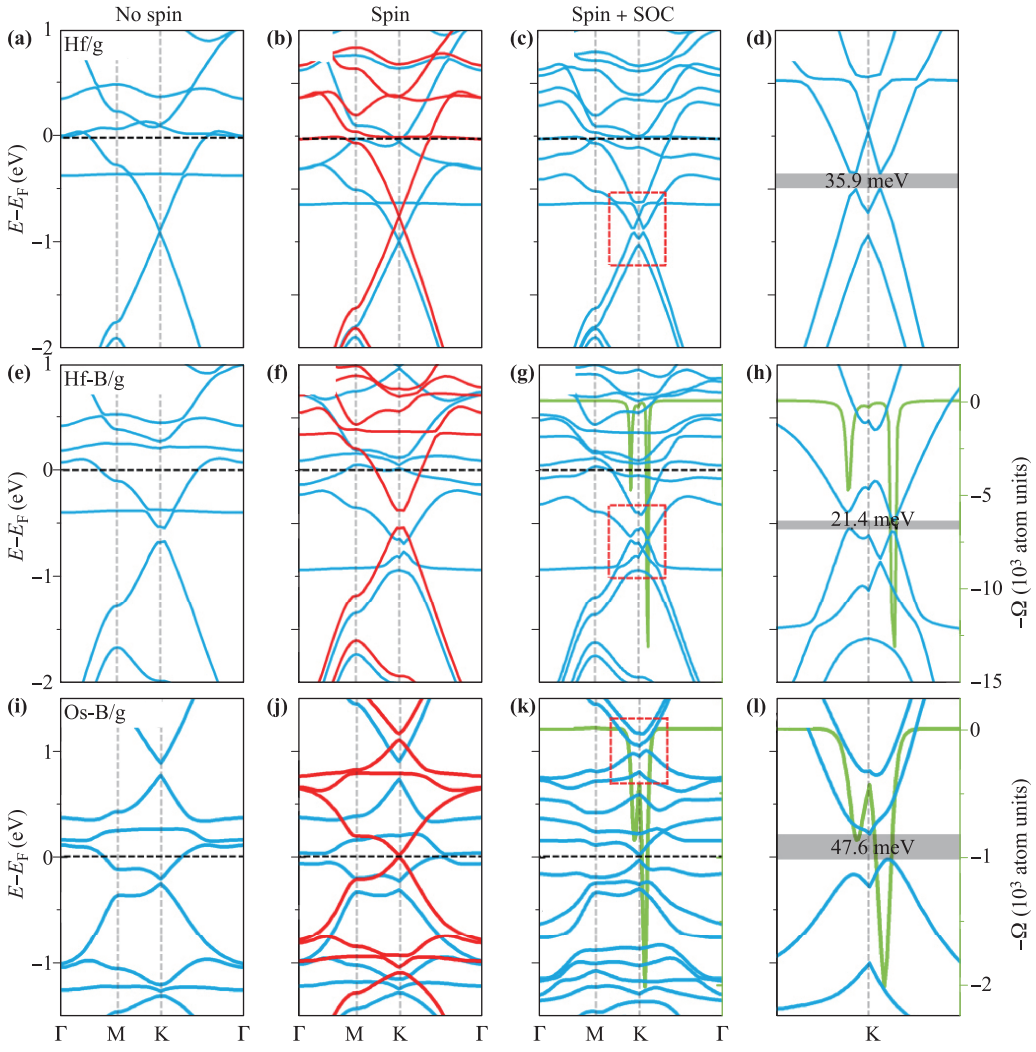

Fig. 3 Band structures of Hf, Hf–B, and Os–B/graphene systems: **(a, e, i)** no spin; **(b, f, j)** without SOC; **(c, g, k)** with SOC. The red and blue lines denote the spin-up and spin-down bands, respectively. The green lines represent the Berry curvature. **(d, h, l)** Magnified views of the red rectangle in (c), (g), and (k), respectively.

doped graphene. In Figs. 4(d) and (h), we show the spin splitting Δ_{SO} for the bands denoted as in Figs. 4(c) and (g) along the highly symmetric line Γ-M-K-Γ. These bands are directly relevant to the transport properties of *n*–*p* co-doped graphene because their band energies are close to the Fermi level. The maximum spin splitting energies are approximately 158 and 85 meV in the Re–B and Pt–B co-doped graphene, respectively, which are much larger than the typical value for the Rashba spin splitting energy in conventional III–V and II–VI semiconductor quantum wells (<30 meV) [53, 54] and are comparable to the enhanced surface Rashba spin splitting energy (∼ 100 meV) in different graphene/substrate systems [21, 22, 25]. Consequently, we conclude that Re–B and Pt–B co-doped graphene would be useful for designing new electronic materials. As for Ta–B, W–B, I–B, and Au–B co-doped graphene systems, their band structures either contain only trivial gaps or lack long-range FM order, indicating that the QAHE cannot be realized with them.

4 Conclusions

In summary, through calculations based on density functional theory, we systematically studied the electronic and spintronic properties of 5*d* TM–B co-doped graphene based on a compensated *n*–*p* co-doping scheme. The electrostatic attraction between the *n*- and *p*-type dopants effectively enhanced the adsorption of the metal adatoms and suppressed their undesirable clustering. The calculated Rashba splitting energies in the Re–B and Pt–B co-

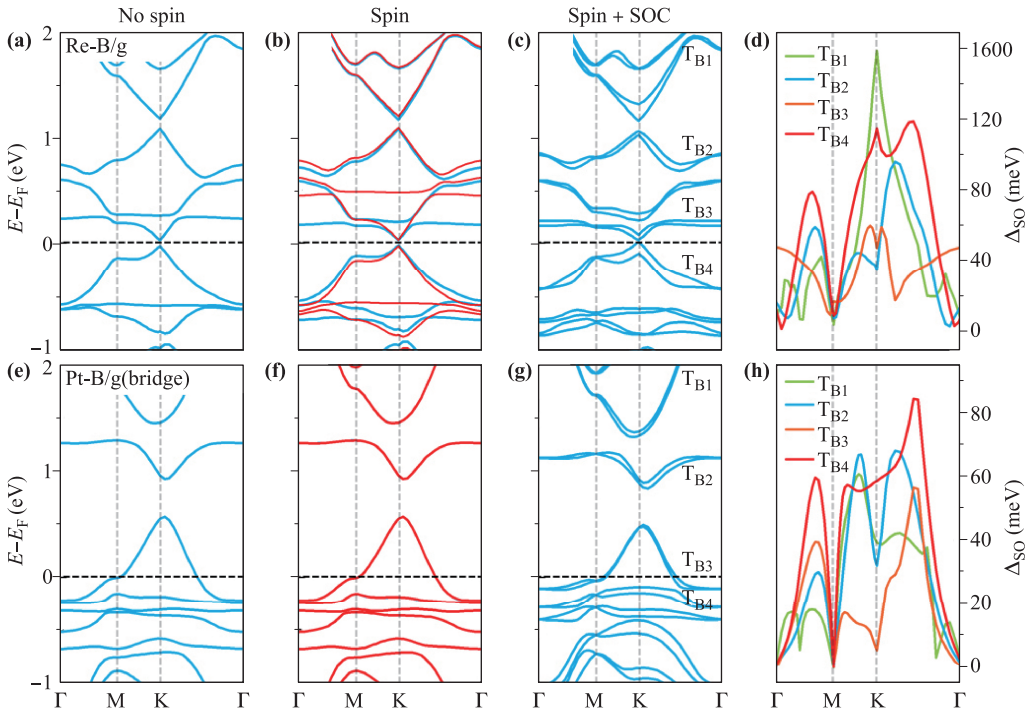

Fig. 4 Band structures of Re–B and Pt–B/graphene systems: **(a, e)** no spin; **(b, f)** without SOC; **(c, g)** with SOC. **(d, h)** Absolute values of spin-orbit (SO) splitting (Δ_{SO}) of T_{B1}-T_{B4} in (c) and (g), respectively.

doped graphene reached 158 and 85 meV, respectively, which are several orders of magnitude larger than the reported intrinsic SOC strength. Moreover, Hf–B and Os–B co-doped graphene can support long-range FM and host the QAHE with non-vanishing Berry curvatures.

Acknowledgements This work was financially supported by the National Key Research and Development Program (Grant No. 2017YFB0405703), the National Natural Science Foundation of China (Grant Nos. 11104173, 61434002, and 51025101) and Sanjin Scholar of Shanxi. X. D. and Z. Q. also acknowledge the support of the China Government Youth 1000-Plan Talent Program and the National Key Research and Development Program (Grant No. 2016YFA0301700). We are grateful to the supercomputing service of AM-HPC and the Supercomputing Center of USTC for providing the high-performance computing resources used in this study.

References

1. F. D. M. Haldane, Model for a quantum Hall effect without Landau levels: Condensed-matter realization of the "Parity anomaly", *Phys. Rev. Lett.* 61(18), 2015 (1988)
2. H. Weng, R. Yu, X. Hu, X. Dai, and Z. Fang, Quantum anomalous Hall effect and related topological electronic states, *Adv. Phys.* 64(3), 227 (2015)
3. Y. F. Ren, Z. H. Qiao, and Q. Niu, Topological phases in two-dimensional materials: A review, *Rep. Prog. Phys.* 79(6), 066501 (2016)
4. C. X. Liu, S. C. Zhang, and X. L. Qi, The quantum anomalous Hall effect: Theory and experiment, *Annu. Rev. Condens. Matter Phys.* 7(1), 301 (2016)
5. C. X. Liu, X. L. Qi, X. Dai, Z. Fang, and S. C. Zhang, Quantum anomalous Hall effect in $Hg_{1-y}Mn_yTe$ quantum wells, *Phys. Rev. Lett.* 101(14), 146802 (2008)
6. R. Yu, W. Zhang, H. J. Zhang, S. C. Zhang, X. Dai, and Z. Fang, Quantized anomalous Hall effect in magnetic topological insulators, *Science* 329(5987), 61 (2010)
7. M. Ezawa, Valley-polarized metals and quantum anomalous Hall effect in silicene, *Phys. Rev. Lett.* 109(5), 055502 (2012)
8. J. Y. Zhang, B. Zhao, and Z. Q. Yang, Abundant topological states in silicene with transition metal adatoms, *Phys. Rev. B* 88(16), 165422 (2013)
9. X. L. Zhang, L. F. Liu, and W. M. Liu, Quantum anomalous Hall effect and tunable topological states in 3d transition metals doped silicene, *Sci. Rep.* 3(1), 2908 (2013)
10. M. Yang, X. L. Zhang, and W. M. Liu, Tunable topological quantum states in three- and two-dimensional materials, *Front. Phys.* 10(2), 108102 (2015)
11. C. C. Liu, J. J. Zhou, and Y. G. Yao, Valley-polarized quantum anomalous Hall phases and tunable topological phase transitions in half-hydrogenated Bi honeycomb monolayers, *Phys. Rev. B* 91(16), 165430 (2015)

12. Z. H. Qiao, S. Y. Yang, W. X. Feng, W.-K. Tse, J. Ding, Y. G. Yao, J. Wang, and Q. Niu, Quantum anomalous Hall effect in graphene from Rashba and exchange effects, *Phys. Rev. B* 82, 161414(R) (2010)
13. Z. H. Qiao, H. Jiang, X. Li, Y. G. Yao, and Q. Niu, Microscopic theory of quantum anomalous Hall effect in graphene, *Phys. Rev. B* 85(11), 115439 (2012)
14. J. Ding, Z. H. Qiao, W. X. Feng, Y. G. Yao, and Q. Niu, Engineering quantum anomalous/valley Hall states in graphene via metal-atom adsorption: An *ab-initio* study, *Phys. Rev. B* 84(19), 195444 (2011)
15. H. B. Zhang, C. Lazo, S. Blügel, S. Heinze, and Y. Mokrousov, Electrically tunable quantum anomalous Hall effect in graphene decorated by 5d transition-metal adatoms, *Phys. Rev. Lett.* 108(5), 056802 (2012)
16. Z. H. Qiao, W. Ren, H. Chen, L. Bellaiche, Z. Y. Zhang, A. H. MacDonald, and Q. Niu, Quantum anomalous Hall effect in graphene proximity coupled to an antiferromagnetic insulator, *Phys. Rev. Lett.* 112(11), 116404 (2014)
17. A. K. Geim and K. S. Novoselov, The rise of graphene, *Nat. Mater.* 6(3), 183 (2007)
18. L. J. Yin, K. K. Bai, W. X. Wang, S. Y. Li, Y. Zhang, and L. He, Landau quantization of Dirac fermions in graphene and its multilayers, *Front. Phys.* 12(4), 127208 (2017)
19. Y. Zhang, Y. W. Tan, H. L. Stormer, and P. Kim, Experimental observation of the quantum Hall effect and Berry's phase in graphene, *Nature* 438(7065), 201 (2005)
20. Y. S. Hor, P. Roushan, H. Beidenkopf, J. Seo, D. Qu, J. G. Checkelsky, L. A. Wray, D. Hsieh, Y. Xia, S. Y. Xu, D. Qian, M. Z. Hasan, N. P. Ong, A. Yazdani, and R. J. Cava, Development of ferromagnetism in the doped topological insulator $Bi_{2-x}Mn_xTe_3$, *Phys. Rev. B* 81(19), 195203 (2010)
21. C. Niu, Y. Dai, M. Guo, W. Wei, Y. Ma, and B. Huang, Mn induced ferromagnetism and modulated topological surface states in Bi_2Te_3, *Appl. Phys. Lett.* 98(25), 252502 (2011)
22. P. P. J. Haazen, J. B. Laloë, T. J. Nummy, H. J. M. Swagten, P. Jarillo-Herrero, D. Heiman, and J. S. Moodera, Ferromagnetism in thin-film Cr-doped topological insulator Bi_2Se_3, *Appl. Phys. Lett.* 100(8), 082404 (2012)
23. T. Jungwirth, J. Sinova, J. Masek, J. Kucera, and A. H. MacDonald, Theory of ferromagnetic (III,Mn)V semiconductors, *Rev. Mod. Phys.* 78(3), 809 (2006)
24. C. Z. Chang, J. Zhang, X. Feng, J. Shen, Z. Zhang, M. Guo, K. Li, Y. Ou, P. Wei, L. L. Wang, Z. Q. Ji, Y. Feng, S. Ji, X. Chen, J. Jia, X. Dai, Z. Fang, S. C. Zhang, K. He, Y. Wang, L. Lu, X. C. Ma, and Q. K. Xue, Experimental observation of the quantum anomalous Hall effect in a magnetic topological insulator, *Science* 340(6129), 167 (2013)
25. J. G. Checkelsky, R. Yoshimi, A. Tsukazaki, K. S. Takahashi, Y. Kozuka, J. Falson, M. Kawasaki, and Y. Tokura, Trajectory of the anomalous Hall effect towards the quantized state in a ferromagnetic topological insulator, *Nat. Phys.* 10(10), 731 (2014)
26. X. Kou, S. T. Guo, Y. Fan, L. Pan, M. Lang, Y. Jiang, Q. Shao, T. Nie, K. Murata, J. Tang, Y. Wang, L. He, T. K. Lee, W. L. Lee, and K. L. Wang, Scale-invariant quantum anomalous Hall effect in magnetic topological insulators beyond the two-dimensional limit, *Phys. Rev. Lett.* 113(13), 137201 (2014)
27. C. Z. Chang, W. Zhao, D. Y. Kim, H. Zhang, B. A. Assaf, D. Heiman, S. C. Zhang, C. Liu, M. H. W. Chan, and J. S. Moodera, High-precision realization of robust quantum anomalous Hall state in a hard ferromagnetic topological insulator, *Nat. Mater.* 14(5), 473 (2015)
28. S. F. Qi, Z. H. Qiao, X. Z. Deng, E. D. Cubuk, H. Chen, W. G. Zhu, E. Kaxiras, S. B. Zhang, X. H. Xu, and Z. Y. Zhang, High-temperature quantum anomalous Hall effect in n–p codoped topological insulators, *Phys. Rev. Lett.* 117(5), 056804 (2016)
29. Y. Ou, C. Liu, G. Y. Jiang, Y. Feng, D. Y. Zhao, W. X. Wu, X. X. Wang, W. Li, C. L. Song, L. L. Wang, W. B. Wang, W. D. Wu, Y. Y. Wang, K. He, X. C. Ma, and Q. K. Xue, Enhancing the quantum anomalous Hall effect by magnetic codoping in a topological insulator, *Adv. Mater.* 30(1), 1703062 (2018)
30. Y. G. Yao, F. Ye, X. L. Qi, S. C. Zhang, and Z. Fang, Spin-orbit gap of graphene: First-principles calculations, *Phys. Rev. B* 75(4), 041401 (2007)
31. M. Gmitra, S. Konschuh, C. Ertler, C. Ambrosch-Draxl, and J. Fabian, Band-structure topologies of graphene: Spin-orbit coupling effects from first principles, *Phys. Rev. B* 80(23), 235431 (2009)
32. A. H. Castro Neto and F. Guinea, Impurity-induced spin-orbit coupling in graphene, *Phys. Rev. Lett.* 103(2), 026804 (2009)
33. J. Hu, J. Alicea, R. Q. Wu, and M. Franz, Giant topological insulator gap in graphene with 5 d adatoms, *Phys. Rev. Lett.* 109(26), 266801 (2012)
34. H. Jiang, Z. Qiao, H. Liu, J. Shi, and Q. Niu, Stabilizing topological phases in graphene via random adsorption, *Phys. Rev. Lett.* 109(11), 116803 (2012)
35. T. Eelbo, M. Waśniowska, P. Thakur, M. Gyamfi, B. Sachs, T. O. Wehling, S. Forti, U. Starke, C. Tieg, A. I. Lichtenstein, and R. Wiesendanger, Adatoms and clusters of 3 d transition metals on graphene: Electronic and magnetic configurations, *Phys. Rev. Lett.* 110(13), 136804 (2013)
36. H. Chen, Q. Niu, Z. Y. Zhang, and A. H. MacDonald, Gate-tunable exchange coupling between cobalt clusters on graphene, *Phys. Rev. B* 87(14), 144410 (2013)
37. J. L. Ge, T. R. Wu, M. Gao, Z. B. Bai, L. Cao, X. F. Wang, Y. Y. Qin, and F. Q. Song, Weak localization of bismuth cluster-decorated graphene and its spin–orbit interaction, *Front. Phys.* 12(4), 127210 (2017)

38. S. F. Qi, H. Chen, X. H. Xu, and Z. Y. Zhang, Diluted ferromagnetic graphene by compensated n–p codoping, *Carbon* 61, 609 (2013)
39. X. Y. Zhang, S. F. Qi, and X. H. Xu, Long-range and strong ferromagnetic graphene by compensated n–p codoping and p–p stacking, *Carbon* 95, 65 (2015)
40. R. Zhang, Y. Luo, S. Qi, and X. Xu, Long-range ferromagnetic graphene via compensated Fe/NO_2 co-doping, *Appl. Surf. Sci.* 305, 768 (2014)
41. X. Z. Deng, S. F. Qi, Y. L. Han, K. H. Zhang, X. H. Xu, and Z. H. Qiao, Realization of quantum anomalous Hall effect in graphene from n–p codoping-induced stable atomic adsorption, *Phys. Rev. B* 95(12), 121410 (2017)
42. T. Yamamoto, H. Katayama, and Yoshida, Solution using a codoping method to unipolarity for the fabrication of p-type ZnO, *Jpn. J. Appl. Phys.* 38(Part 2, No. 2B), L166 (1999)
43. L. G. Wang and A. Zunger, Cluster-doping approach for wide-gap semiconductors: The case of p-type ZnO, *Phys. Rev. Lett.* 90(25), 256401 (2003)
44. Y. Gai, J. B. Li, S. S. Li, J. B. Xia, and S. H. Wei, Design of narrow-gap TiO_2: A passivated codoping approach for enhanced photoelectrochemical activity, *Phys. Rev. Lett.* 102(3), 036402 (2009)
45. W. G. Zhu, X. F. Qiu, V. Iancu, X. Q. Chen, H. Pan, W. Wang, N. M. Dimitrijevic, T. Rajh, M. P. Meyer, G. M. Paranthaman, H. H. Stocks, B. H. Weitering, G. Gu, Eres, and Z. Y. Zhang, Band gap narrowing of titanium oxide semiconductors by noncompensated anion-cation codoping for enhanced visible-light photoactivity, *Phys. Rev. Lett.* 103(22), 226401 (2009)
46. X. H. Xu, H. J. Blythe, M. Ziese, A. J. Behan, J. R. Neal, A. Mokhtari, R. M. Ibrahim, A. M. Fox, and G. A. Gehring, Carrier-induced ferromagnetism in n-type ZnMnAlO and ZnCoAlO thin films at room temperature, *New J. Phys.* 8(8), 135 (2006)
47. W. G. Zhu, Z. Y. Zhang, and E. Kaxiras, Dopant-assisted concentration enhancement of substitutional Mn in Si and Ge, *Phys. Rev. Lett.* 100(2), 027205 (2008)
48. S. Agnoli and M. Favaro, Doping graphene with boron: A review of synthesis methods, physicochemical characterization, and emerging applications, *J. Mater. Chem. A* 4(14), 5002 (2016)
49. P. E. Blöchl, Projector augmented-wave method, *Phys. Rev. B* 50(24), 17953 (1994)
50. G. Kresse and J. Hafner, *Ab initio* molecular-dynamics simulation of the liquid-metal–amorphous-semiconductor transition in germanium, *Phys. Rev. B* 49(20), 14251 (1994)
51. Y. G. Yao, L. Kleinman, A. H. MacDonald, J. Sinova, T. Jungwirth, D. S. Wang, E. Wang, and Q. Niu, First principles calculation of anomalous Hall conductivity in ferromagnetic bcc Fe, *Phys. Rev. Lett.* 92(3), 037204 (2004)
52. D. Xiao, M. C. Chang, and Q. Niu, Berry phase effects on electronic properties, *Rev. Mod. Phys.* 82(3), 1959 (2010)
53. G. Kresse and J. Hafner, *Ab initio* molecular dynamics for liquid metals, *Phys. Rev. B* 47(1), 558 (1993)
54. G. Kresse and J. Furthmüller, Efficiency of ab-initio total energy calculations for metals and semiconductors using a plane-wave basis set, *Comput. Mater. Sci.* 6(1), 15 (1996)
55. J. P. Perdew, K. Burke, and M. Ernzerhof, Generalized gradient approximation made simple, *Phys. Rev. Lett.* 77(18), 3865 (1996)
56. J. P. Perdew, K. Burke, and M. Ernzerhof, Generalized gradient approximation made simple [*Phys. Rev. Lett.* 77, 3865 (1996)], *Phys. Rev. Lett.* 78(7), 1396 (1997)